Journal of
Composites Science

MDPI

Article

Structure Formation Mechanisms in Wet and Dry Pellets of the "Clay Mineral–Iron Ore Concentrate" Composite System

Yevhen Chuprinov [1], Kateryna Shmeltser [1], Inna Trus [2], Denis Miroshnichenko [3,4,*], Liudmyla Lysenko [3,4], Andriy Myronenko [3], Mariia Shved [5] and Nataliia Hrudkina [6]

[1] The Department of Metallurgical Technology, State University of Economics and Technology, 50005 Kriviy Rih, Ukraine; chuprynov_yv@duet.edu.ua (Y.C.); shmeltser@duet.edu.ua (K.S.)
[2] Department of Ecology and Plant Polymer, Technologies National Technical University of Ukraine "Igor Sikorsky Kyiv Polytechnic Institute", 03056 Kyiv, Ukraine; inna.trus.m@gmail.com
[3] The Department of Oil, Gas and Solid Fuel Refining Technologies, National Technical University «Kharkiv Polytechnic Institute», 61002 Kharkiv, Ukraine; liudmylalysenko73@gmail.com (L.L.); 4norim@gmail.com (A.M.)
[4] The Coal Department, Ukrainian State Research Institute for Carbochemistry, 61023 Kharkiv, Ukraine
[5] Department of Information Protection, Lviv Polytechnic National University, 79013 Lviv, Ukraine; mariia.y.shved@lpnu.ua
[6] Department of Natural Sciences and General Engineering Disciplines, Technical University "Metinvest Polytechnic", 69008 Zaporizhzhia, Ukraine; n.s.grudkina@mipolytech.education
* Correspondence: denys.miroshnychenko@khpi.edu.ua

Abstract

This article examines the interaction of clay minerals with iron ore concentrate in the context of the efficient use of composite mineral resources. The role of the adsorption properties of mineral additives in the formation of interparticle bonds in green pellets is analyzed. Using X-ray diffraction (XRD) and infrared spectroscopy, the dehydration processes of Na- and Ca-montmorillonite were investigated, and the influence of the cation type on the minerals' ability to retain water was established. The high thermal stability of the structural OH groups of montmorillonite from the IV-layer clay of the Cherkasy deposit was confirmed, which is an important factor during high-temperature processing of mineral raw materials. Electron microscopy results showed that the fourth-layer clay forms an optimal porous composite microstructure, which contributes to increased water-holding capacity and gas permeability of the pellets. A direct correlation between the adsorption capacity of mineral additives and the strength of raw and dried pellets was experimentally confirmed. Montmorillonite with palygorskite from Layer IV, characterized by high adsorption capacity and prolonged dehydration processes, was identified as the most effective composite binding additive. The results obtained deepen scientific understanding of the mechanisms underlying pellet strength formation and have practical significance for the rational and resource-efficient use of mineral resources in the production of iron ore pellets. The results also demonstrate the potential for improving resource efficiency in pellet production through reduced consumption of traditional binder materials.

Keywords: metallurgical production; iron ore pellets; adsorption capacity; dehydration; pellet strength; montmorillonite; palygorskite; composite binding additive

Academic Editor: Guoqiang Xie

Received: 7 April 2026
Revised: 29 April 2026
Accepted: 7 May 2026
Published: 11 May 2026

1. Introduction

1.1. Literary Review

Iron ore pellets are a key component of modern blast furnace burden [1–3], ensuring stable gas permeability, uniform reduction behavior, and high metallurgical efficiency. The mechanical strength of both green and fired pellets directly affects their resistance to degradation during transportation, drying, and high-temperature processing. Therefore, improving pellet strength remains a critical technological task in iron ore agglomeration.

During pellet formation, binder additives play a decisive role in the development of interparticle cohesion. They influence green pellet formation, drying stability, resistance to cracking, and final mechanical properties. Industrially, bentonite remains the most widely used inorganic binder due to its swelling capacity, adsorption properties, and ability to form stable capillary bridges between iron ore particles.

The mechanisms by which bentonite strengthens pellets are commonly explained by capillary forces, fiber formation, and the hydration of montmorillonite layers. The adsorption capacity of clay minerals governs water retention, interlayer swelling, and dehydration behavior, which in turn influence pellet structure formation. Previous studies have qualitatively described these mechanisms; however, quantitative relationships between adsorption thermodynamics, dehydration kinetics, and pellet mechanical strength remain insufficiently established.

Despite extensive investigations of bentonite binders in iron ore pelletization, a direct statistical correlation between adsorption capacity and pellet strength has not been systematically demonstrated. In addition, the influence of mineralogical heterogeneity, particularly montmorillonite-palygorskite mixtures, on dehydration behavior and microstructural evolution remains unclear.

The objective of this study is to establish quantitative relationships among adsorption capacity, dehydration characteristics, microstructure formation, and the mechanical strength of green and dry pellets, with particular emphasis on montmorillonite-palygorskite systems.

The improvement of the blast furnace process today covers a wide range of technological solutions—from optimizing the blowing parameters and using natural gas substitutes to implementing intelligent smelting control systems. However, one of the most important areas remains the high-quality preparation and modernization of charge materials, since their properties determine the stability of the gas-dynamic regime of the furnace. In this context, special attention is paid to coke, which serves not only as a fuel and reducing agent but also provides drainage capacity in the lower furnace zones. Improving the strength characteristics of coke and controlling its reactivity can significantly reduce specific fuel consumption and increase unit productivity, making the entire process more cost-effective and environmentally friendly [4–8].

In addition to coke quality, the preparation of the iron-bearing components of the burden is equally critical to blast furnace stability. In modern practice, iron ore pellets constitute a significant share of the burden and largely determine gas permeability, reduction uniformity, and resistance to mechanical degradation during charging and high-temperature processing. Therefore, alongside coke optimization, improving the physicochemical properties and mechanical strength of iron ore pellets represents a fundamental direction in the development of efficient agglomeration technologies.

Binder additives in the processes of obtaining iron ore pellets perform important technological functions and should have the following multifactorial positive impact on the technology of their production: to maximally preserve the iron content obtained during ore enrichment; to improve the agglomeration of the charge; to reduce, if necessary, its humidity to the optimal value; to improve the structure and strength characteristics of

raw pellets, in the processes of their drying, heating and firing, as well as finished fired pellets [9].

By their composition, binders are divided into two groups: inorganic (mineral) and organic [9]. Commonly used inorganic binders in industrial production include bentonite clay and activated lime (quicklime or slaked) [10]. In recent decades, organic binders have included sodium carboxymethylcellulose, "peridur", technical lignosulfonate, sulfite-alcohol bard, etc. [11]. The amount of bentonite clay in the mixture is (by dry mass) 0.15–1.0%, lime—2–5% [9]. The amount of organic binders in the mixture is 0.05–0.1%, i.e., an order of magnitude lower than bentonite clay [12].

In most pellet-producing enterprises, bentonite clay is practically the only binding additive, as it best meets the above-mentioned technological requirements [13].

The structure of montmorillonite is a three-layer stack: two layers of silicon-oxygen tetrahedra, facing each other with their vertices, are sandwiched between layers of aluminum-hydroxyl octahedra [14]. The thickness of the elementary package is 0.96 nm. The properties of the montmorillonite crystal are not constant and depend on ion exchange reactions in the tetrahedral and octahedral layers.

In tetrahedra, it is possible to replace Si^{4+} with Al^{3+}, in octahedra, with Al^{3+} and Fe^{3+} with Mg^{2+}. The replacement of cations in tetrahedra and octahedra with ions of lower valence leads to the fact that the elementary layers acquire a negative charge. The negative charge is compensated by positively charged ions, which in turn attract the next packet.

Thus, a clay particle, then an aggregate of clay particles, is formed. In the gap between the montmorillonite packets, metal cations (Na^+, Li^+, K^+, Ca^{2+}, Mg^{2+}) are located, which balance the negative charge of the layers. Depending on the predominance of one exchange cation, for example, Na^+, or a group of cations (Ca^{2+}, Mg^{2+}), sodium and calcium-magnesium montmorillonites are found in nature, respectively.

As a result of the entry of molecular water into the interlayer space, the mineral particles swell. The alkali metal ions (Na^+ and K^+) and, primarily, Na^+ have the greatest hydration capacity. The alkaline earth metal ions (Ca^{2+} and Mg^{2+}) have a significantly lower hydration capacity [15–18].

Alkaline earth bentonites are characterized by lower hydrophilicity and binding capacity, and are usually inferior in quality to alkaline bentonites [19].

Alkaline earth bentonites, when modified using the developed technology with sodium preparations (at 2–5% of the bentonite's dry mass), are converted into alkaline bentonites, retaining their inherent characteristics and properties. Modified alkaline-earth bentonites are also widely used in the production of iron ore pellets [20].

Highly swelling bentonites that form viscous porous suspensions [21,22], under otherwise identical agglomeration conditions, provide the formation of pellets with higher humidity, strength during the drying process and after drying [23], and also withstand a higher limit drying temperature (shock) due to the gradual removal of moisture from the interlayer space of the montmorillonite lattice [24]; increased nucleation in the system due to the fact that less pore liquid is released on the surface of the granules during their formation, which allows for a higher yield of a suitable pellet class at a higher charge humidity; the manifestation of positive results for the process of obtaining raw pellets, especially for charges with increased humidity, at a 25–30% lower consumption of these bentonites compared to weakly swelling alkaline earth bentonites [25].

The main disadvantage of low-swelling alkaline-earth bentonite clays is their increased sensitivity to over-wetted mixtures, especially to fluctuations in moisture content at higher moisture levels. Obtaining a concentrate with optimal moisture content and minimal fluctuations will enable the use of alkaline-earth bentonites in pellet production, expanding their raw material base and reducing the cost of finished products [26].

The positive and negative effects of modified alkaline bentonite clays on the agglomeration process of iron ore concentrates, as well as the characteristics of raw and calcined pellets, are similar to those of natural alkaline bentonites and can replace them in pellet production without deterioration of technological performance [27].

Modern research emphasizes that bentonite remains the primary binder in pellet production due to its high availability, low cost, and proven application technology [28]. To improve the industrial characteristics of raw materials, such as Egyptian bentonite, the hydrocyclone separation method is effective, preserving the montmorillonite structure and increasing the pellets' strength after thermal hardening [29]. Bentonite is also considered an ecological additive in cement mixtures, where it reduces the heat of hydration and moisture absorption, although its effect on the overall mechanical strength of the product remains a subject of scientific debate [30].

The effectiveness of bentonite as a binder is also compared with that of organic and industrial wastes, such as spent paper industry solutions, which contain sodium and calcium [31]. Purified bentonite improves thermal hardening of pellets, thereby promoting the formation of strong bridges through diffusion processes [28]. In a comparative analysis with new organic binders such as pectin or CMC, bentonite demonstrates consistently high strength, particularly after high-temperature firing, which is critical for subsequent redistribution in blast furnaces [32].

1.2. Research Gap and Hypothesis

Despite extensive investigations of bentonite binders in iron ore pelletization, particularly in the works of Forsmo et al. [18–20] and Kawatra et al. [10,11,13,18,24,25,27], the binding mechanisms are predominantly interpreted through qualitative descriptions of capillary forces and fiber formation. However, several aspects remain insufficiently clarified.

First, the quantitative relationship between the adsorption capacity of clay minerals and the mechanical strength of green and dried pellets has not been systematically established. Existing studies describe hydration and fiber bonding mechanisms but do not provide a direct statistical correlation between adsorption thermodynamics and pellet strength parameters.

Second, the influence of mineralogical heterogeneity within natural bentonite deposits, especially the presence of palygorskite in mixed-layer systems, on the dehydration kinetics and structural stability during pellet drying has not been thoroughly investigated.

Third, the staged mechanism of strength development in the "clay mineral—iron ore concentrate" system (green state—drying—heating) lacks a unified conceptual model that integrates adsorption, capillary pressure evolution, microstructure formation, and thermal stability.

Therefore, the scientific gap addressed in this work is the establishment of a quantitative, mechanistically grounded relationship between adsorption capacity, dehydration behavior, microstructure evolution, and mechanical strength of pellets, with particular emphasis on montmorillonite–palygorskite systems.

The working hypothesis of the study is that the adsorption capacity and extended dehydration interval of montmorillonite containing palygorskite result in a statistically significant increase in both green and dry pellet strength, due to prolonged capillary cohesion and improved microstructural organization.

This study provides a quantitative link between the adsorption capacity of clay minerals and pellet mechanical strength, combining mineralogical characterization (XRD, IR spectroscopy, SEM, and BET) with statistical analysis of pellet strength. Unlike previous pelletization studies, which primarily describe binder mechanisms qualitatively through

capillary and fiber bonding concepts, the present work establishes a statistically significant correlation between adsorption energy and pellet strength ($R^2 > 0.96$).

The novelty of the research lies in three key aspects: the direct correlation between adsorption energy and both green and dry pellet strength; the identification of the synergistic role of montmorillonite–palygorskite mixtures in extending the dehydration interval; and the microstructural explanation of pellet strengthening based on quantitative SEM analysis and porosity evaluation.

The results have clear industrial relevance, providing a mechanistically grounded basis for optimizing binder selection and reducing bentonite consumption in large-scale iron ore pellet production.

It should be emphasized that the present study focuses on the mechanisms of structure formation and strength development at the stages of green pellet formation and subsequent drying. The high-temperature roasting stage, including solid-phase reactions, diffusion bonding, and recrystallization processes between iron oxides and binder phases, is beyond the scope of this work. These processes involve fundamentally different physicochemical mechanisms and require separate investigation using high-temperature experimental techniques and phase transformation analysis. Therefore, the conclusions drawn in this study are limited to low- and intermediate-temperature stages of pellet formation.

2. Materials and Methods

Research Methodology

To expand our understanding and obtain new scientific data on the properties of different forms of bentonite, samples of activated (Na-form, Figure 1) bentonite of Greek origin (Milos Island, Greece) and bentonite of the 2nd layer of the Cherkasy deposit, Ukraine (Ca-form, Figure 2) were analyzed by X-ray diffraction (XRD) [33,34]. This method is a tool for studying the mineralogical composition and structural changes in clay minerals.

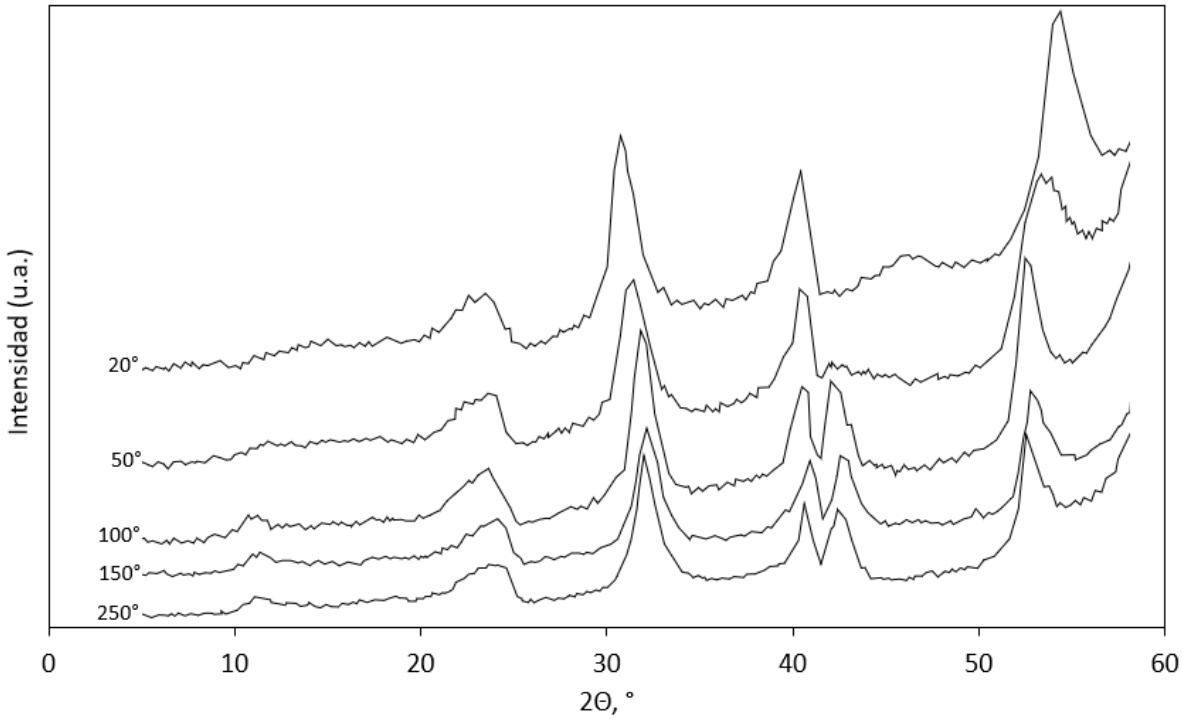

Figure 1. Dehydration diffraction pattern of activated (Na-form) bentonite of Greek origin.

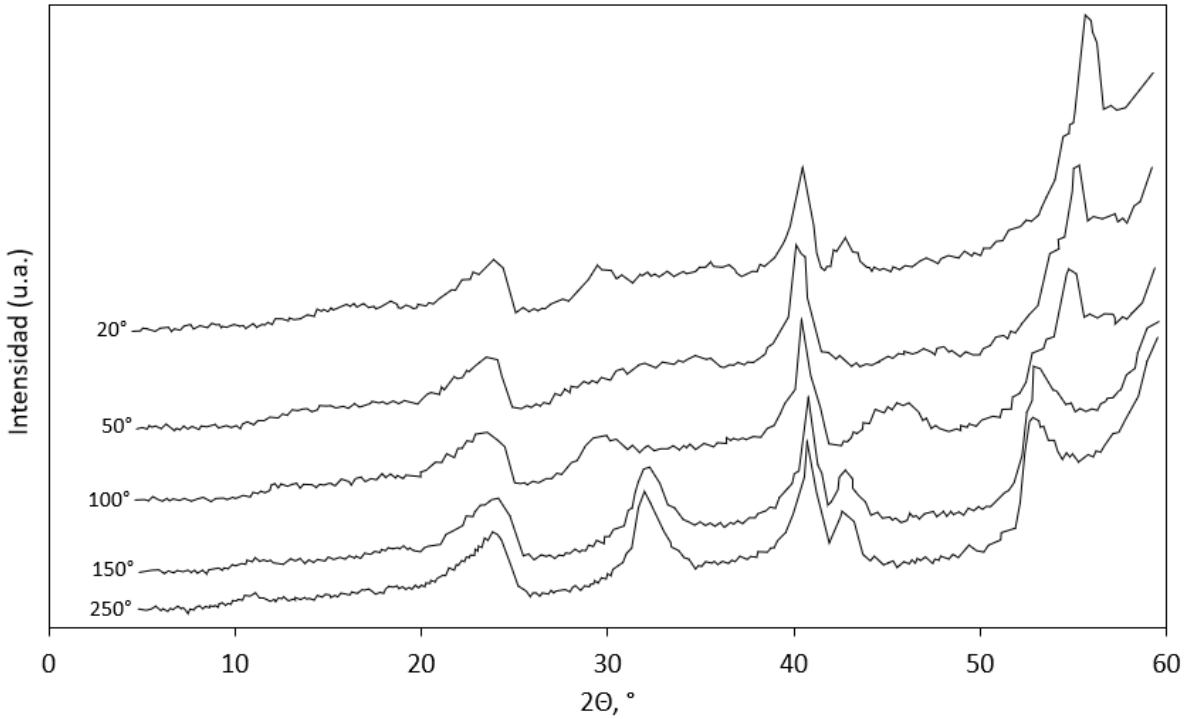

Figure 2. Diffractogram of dehydration of bentonite of the 2nd layer of the Cherkasy deposit (Ca-form).

XRD measurements were carried out using a CuKα radiation source (λ = 1.5406 Å) operating at 40 kV and 30 mA. The scanning range was 3–60° 2θ with a step size of 0.02° and a scanning speed of 2°/min. The samples were analyzed in air-dried and thermally treated states. Phase identification and peak fitting were performed using HighScore Plus software (version 4.9) with reference to the PDF-4 database.

The study of adsorption capacity was conducted in the technical laboratory of PJSC "ArcelorMittal Kryvyi Rih". Clays from the Cherkasy deposit (montmorillonite of layers II and IV) and kaolinite were selected as binding additives, and a variant without binding additives was considered.

Adsorption capacity (A, J/g) is defined as the amount of energy associated with the adsorption of water molecules per unit mass of material, determined under controlled laboratory conditions. It reflects the ability of the binder to retain moisture and form stable hydration layers, which are critical for capillary bonding during pellet formation.

To study the processes of pelletization in the laboratory conditions of the Educational and Scientific Technological Institute, the concentrate of the ore enrichment plant No. 2 of PJSC "ArcelorMittal Kryvyi Rih" (Fe content = 65.3%) was used. The iron ore concentrate was sieved, leveled on a metal sheet, moistened to 9% humidity (basic), mixed, sieved again, and stored in a desiccator for 24 h. To determine the moisture content of the charge, which ensures the maximum yield of suitable pellets, undissolved and overmoistened by 0.5% (8.5% and 9.5%, respectively) concentrates were prepared in the same way [34].

In parallel, the binding additives were prepared, dried in a drying oven at 105 °C, ground in a laboratory mill (Figure 3), and stored in a desiccator.

Figure 3. Laboratory mill.

The moistened concentrate sample, which had been kept in the desiccator, was again placed on a metal sheet and leveled. 0.5% of the binder additive (see Table 1) was evenly dosed onto the leveled surface of the concentrate (based on the weight of the dry concentrate), mixed until traces of the binder disappeared, passed through a sieve into the desiccator, and kept for 30 min before pelleting.

Table 1. Results of pelletizing pellets with different binder additives.

Type of Binder	Strength Index, kg/pell			
	Raw Pellets		Dried Pellets	
Without binder	1.1 1.2 1.1	1.1 *	2.2 2.4 2.3	2.3 *
Kaolinite	1.4 1.3 1.3	1.3 *	3.7 3.7 3.9	3.8 *
Montmorillonite II layer	1.5 1.5 1.5	1.5 *	5.9 5.9 5.9	5.9 *
Montmorillonite IV layer	1.6 1.7 1.8	1.7 *	6.4 6.2 6.2	6.3 *

* arithmetic mean for three experiments (20 pellets in each).

The calculation of the number of pellet seed aggregates was carried out according to the equation:

$$Q = \frac{m}{5}, \quad (1)$$

where Q is the number of pellet seed aggregates, pieces; m is the mass of the agglomerated charge, g; 5 is the approximate mass of one raw pellet, g.

One-fifth of the wet mixture was loaded into the pelletizer (Figure 4), which rotated at 40 rpm.

Figure 4. Laboratory disc pelletizer.

To obtain embryos with a diameter of 4–5 mm, water was supplied to the mixture using a spray gun. The finished embryos were separated from the remaining mixture in the pelletizer, and the required amount was counted according to Equation (1). The remaining embryos were kneaded and mixed with the bulk of the mixture. Then, the remaining mixture was rolled onto the selected embryos, evenly loading portions into the pelletizer every 10 s.

The mixture was pelletized for 10 min. The obtained pellets had a diameter of 10–12 mm, which corresponds to the typical industrial size fraction for blast furnace pellets. The size distribution was controlled by manual screening, and only pellets within this diameter range were selected for strength testing.

Modeling the continuity of the pelleting regime was achieved by continuous, strictly timed, portioned dosing of the charge onto previously obtained pellet nuclei of 4–5 mm in size, the number of which was calculated. The impact of charge humidity was assessed based on pellet quality indicators.

Drying of green pellets was carried out in a laboratory drying oven at 105 °C for 60 min under an air atmosphere. After drying, the pellets were cooled to room temperature in a desiccator to prevent moisture reabsorption prior to mechanical testing.

Pellet compressive strength was measured using a laboratory universal testing machine under uniaxial compression. The loading rate was set to 5 mm/min. The maximum force at pellet fracture was recorded and expressed in kg/pellet. For each experimental condition, 20 randomly selected pellets were tested. Each experiment was repeated three times (total $n = 60$), and the reported values represent arithmetic means.

Statistical analysis was performed using linear regression to evaluate the relationship between adsorption capacity and pellet strength. The coefficient of determination (R^2) was calculated to assess the strength of the correlation. Differences between binders were evaluated using Student's t-test at a significance level of $p < 0.05$. Standard deviations were calculated for each dataset.

3. Results

3.1. X-Ray Diffraction Analysis of Bentonite Clay Samples

The main work of adhesion of concentrate particles is provided by the forces of capillary pressure of water adsorption films in intergranular pores. The role of the binder additive particles during this period is reduced only to increasing the effective surface, which, with great force and in a much larger quantity than the concentrate surface, keeps water molecules in the adsorption state. In other words, the surface of clay particles, having a much higher adsorption capacity compared to the surface of ore mineral particles, creates additional excess capillary pressure in the pores, where the distance between the walls of the capillaries formed by opposite faces of magnetite crystals exceeds the thickness of 4–6 layers of water molecules. In such pores, layered crystals of clay minerals form capillary vessels with heterogeneous walls, one of which—magnetite—is wetted weaklier than the other—montmorillonite, but with a total energy somewhat greater than if both walls were only magnetite.

Another function of the strengthening additive during the initial period of agglomeration of concentrate particles is to provide additional moisture during the drying process, instead of the removed pore water associated only with the outer surface of the ore and clay mineral particles.

The diffractogram shows five curves, each corresponding to a specific temperature (20°, 50°, 100°, 150°, 250°). The main change in hydration of the clay mineral that attracts attention occurs in the low-angle region (up to 10–15° 2θ), where the basal reflex (001) of montmorillonite is located. This peak is most sensitive to the water content in the clay's interlayer space. With increasing temperature, this peak shifts to higher 2θ angles and decreases in intensity, indicating the loss of interlayer water and the compression of the crystal lattice. Peaks at higher 2θ angles (e.g., around 23–26° and 40–50°) likely correspond to other impurities (e.g., quartz, feldspars) or internal reflections of montmorillonite (e.g., (020) or (110) reflections), which are less susceptible to dehydration.

At 20 °C (initial state), the band in the low-angle region (about 5–6° 2θ) is the most intense and broadest. This corresponds to the most hydrated state of Na-montmorillonite with the largest interlayer distance (d001). A typical d001 distance for hydrated Na-montmorillonite is about 13–15 Å, corresponding to 2θ angles of 5.8–6.8° (according to the Bragg equation).

With increasing temperature to 50 °C and 100 °C, the 001 peak shifts noticeably to the right (to larger 2θ), indicating a decrease in the interlayer distance. This is due to the removal of weakly bound (sorbed) water, which is located in the outer layers of water molecules between the montmorillonite packets. The hydration and dehydration process of montmorillonite is reversible at temperatures up to 100 °C [35].

At 150 °C, the peak continues to shift, and its intensity may decrease. This indicates further water loss, including partial removal of more tightly bound water that interacts with interlayer Na^+ cations.

At 200–250 °C, the 001 peak shifts to the maximum 2θ values within the observed range (probably around 7–8° 2θ). This indicates a significant compression of the interlayer space due to the removal of almost all interlayer water, including tightly bound water. At these temperatures, montmorillonite enters a dehydrated state. According to studies, the c-parameter (crystal lattice parameter) of montmorillonite decreases with increasing heat treatment temperature due to dehydration [36,37].

Peaks located at higher 2θ angles (e.g., around 26–28° for quartz or other minerals, and diffuse peaks for amorphous phases or less ordered parts of the structure) remain relatively stable in their position or change in intensity only slightly. This confirms that dehydration

mainly affects the interlayer space of montmorillonite, while the main tetrahedral and octahedral layers and other crystalline impurities retain their structure.

The type of interlayer cation (Na^+ versus Ca^{2+}) significantly affects the hydration properties of montmorillonite and, consequently, its dehydration [38].

For the Ca-form, as for Na-bentonite, the least significant changes occur in the low-angle region (up to 20° 2θ), where the basal reflection (001) of montmorillonite is located (See Figure 2). However, compared to the Na-form, the initial position of this peak (at 20 °C) and its behavior upon heating will differ due to the influence of the Ca^{2+} cation.

Ca^{2+} cations are divalent, have a smaller hydration radius and a larger charge compared to monovalent Na^+. This leads to the conclusion that Ca^{2+} interacts more strongly with water molecules and the montmorillonite surface than Na^+. As a result, Ca-montmorillonite usually has a smaller initial interlayer distance (d001) in the hydrated state compared to Na-montmorillonite and requires higher temperatures to completely remove interlayer water.

In contrast to the Na-form (where the 001 peak was around 5–6° 2θ), for Ca-bentonite, the main basal peak (001) is located in the region of approximately 7–8° 2θ. This corresponds to an interplanar distance of about 10–12 Å, which is typical for Ca-montmorillonite with a single layer of water molecules or a partially hydrated state. This confirms that Ca-montmorillonite is less hydrated than the Na-form under the same conditions.

At 50 °C, the (001) peak shows a slight shift to the right (i.e., to higher 2θ). This indicates that removing weakly bound water from Ca-bentonite requires slightly higher temperatures, or that the initial amount of such water is smaller. The changes at this stage are less pronounced than in the Na-form.

At 100 °C, a more pronounced but still moderate shift in the (001) peak to the right (to larger 2θ) is observed, indicating further removal of interlayer water. At this stage, a significant portion of the interlayer water is lost.

At 150 °C, the (001) peak continues to shift to the right, becoming more diffuse and less intense. This indicates intense dehydration and further compression of the interlayer space. The interlayer distance decreases, approaching the size of dry montmorillonite.

At 250 °C, the (001) peak shifts to the maximum 2θ values in this series. This indicates a state close to complete dehydration of the interlayer space. The interplanar distance decreases to minimum values (about 9–10 Å for dehydrated montmorillonite). Compared to the Na-form, which already at 250 °C has a strongly compressed, sometimes barely noticeable peak, the Ca-form can still retain a more pronounced, albeit shifted, reflex, demonstrating stronger water retention.

Peaks at larger 2θ angles (e.g., around 26–28° and 40–50°), which correspond to internal reflections of montmorillonite or mineral impurities (e.g., quartz), remain relatively stable in their position. Their intensity also changes slightly. This confirms that dehydration mainly affects the interlayer space and its associated water molecules, without destroying the underlying structure of the clay mineral layers or the impurities in this temperature range.

Water molecules are removed from the interlayer spaces of montmorillonite up to 180 °C (from the Na-form)—220 °C (from the Ca-form), from the structural channels of palygorskite—in two stages: 120–180 °C and 250–360 °C. These molecules, diffusing from the structure into the porous space, then along the pore walls and capillaries, continue to perform the work of particle adhesion.

Therefore, one important condition for regulating water release by a binder additive is to expand the temperature range of dehydration, which can be achieved by introducing palygorskite into the charge. As shown by the IR spectra (Figure 5) of the dehydration of Dash-Salakhlin and Cherkasy montmorillonites and a natural mixture of montmorillonite

with palygorskite (layer IV), this process takes the longest, almost up to 400 °C, in the presence of palygorskite, which is reflected in electron microscopic images (Figure 6).

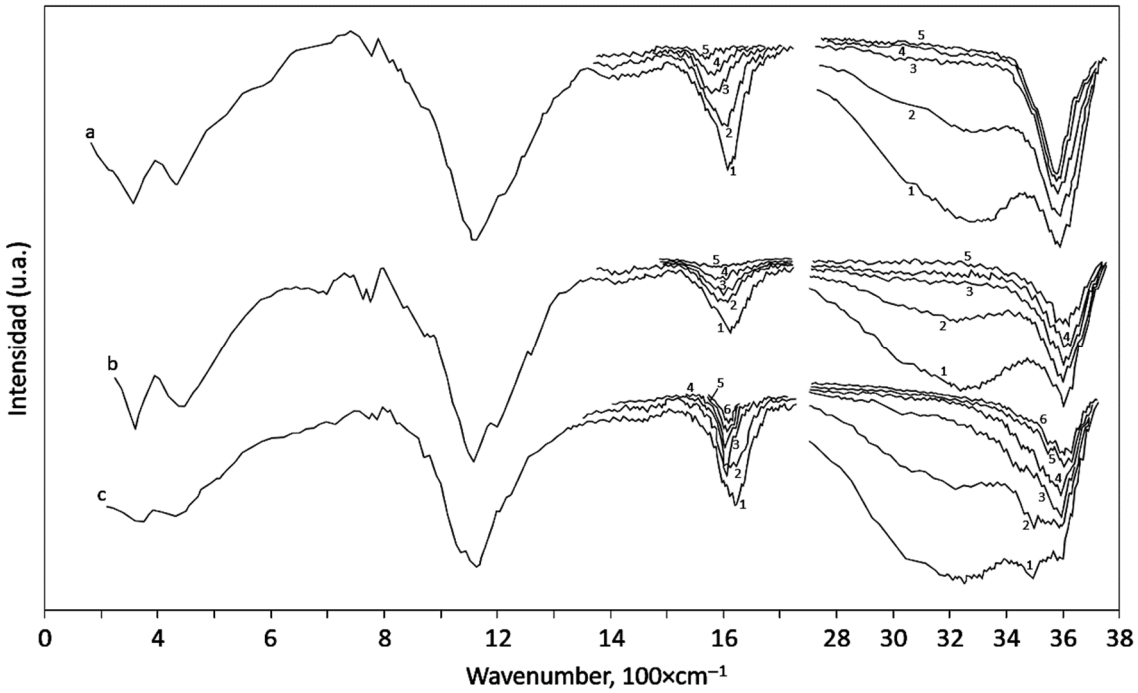

Figure 5. Infrared spectra of dehydration of Dash-Salakhlin bentonite (a), Cherkasy bentonite of the II layer (b), and montmorillonite clay of the IV layer of the Cherkasy deposit (c): 1—20 °C, 2—50 °C, 3—100 °C, 4—200 °C, 5—300 °C, 6—340 °C.

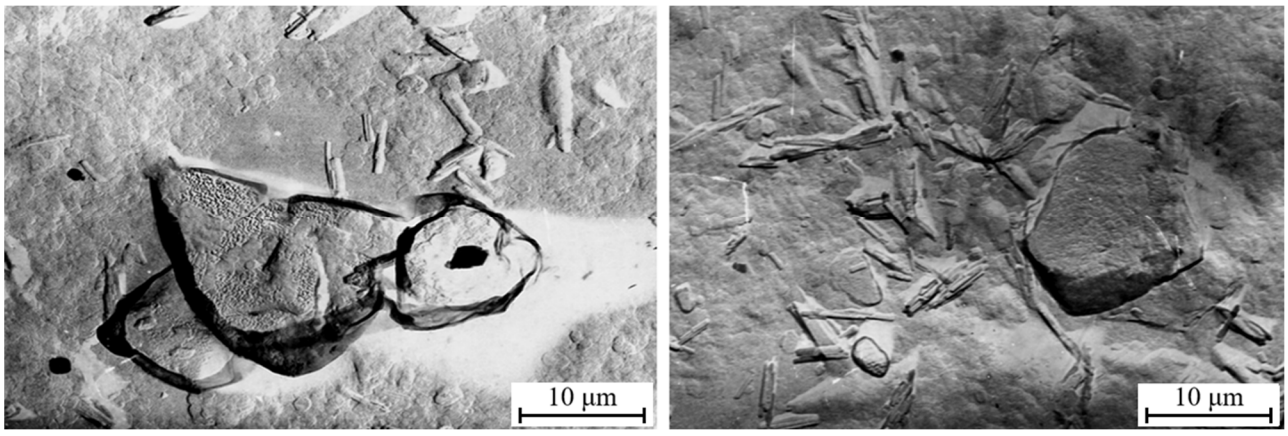

(**a**) (**b**)

Figure 6. Electron microscopic images of artificial clay mixtures of the Cherkasy deposit: (**a**)—layer II + layer III: (**b**)—layer II + layer IV.

Figure 5 contains infrared spectra of three different samples of clay materials—Dash-Salakhlin bentonite (a), Cherkasy bentonite of the II layer (b) and montmorillonite clay of the IV layer of the Cherkasy deposit (c)—that were subjected to dehydration at different temperatures: 20 °C, 50 °C, 100 °C, 200 °C, 300 °C and 340 °C. Infrared spectroscopy (IR spectroscopy) allows detailed monitoring of changes in molecular vibrations and functional groups during dehydration, particularly the loss of adsorbed, interlayer, and structural water.

Analyzing the high-frequency region of the spectra (3800–3000 cm^{-1}), which corresponds to the stretching vibrations of OH groups, and the region of deformation vibrations

of water (~1630–1640 cm^{-1}), it is possible to trace the dynamics of dehydration. In all three samples, significant decreases in peak intensity at ~3400 cm^{-1} and ~1630 cm^{-1} are observed with increasing temperature from 20 °C to 200 °C. This indicates the effective removal of adsorbed and weakly bound interlayer water, a characteristic of montmorillonites.

However, the key difference between the samples lies in the thermal stability of the structural OH groups, as reflected by a peak at about 3600 cm^{-1}. For Dash-Salakhlin bentonite (see Figure 5a) and Cherkasy bentonite of the II layer (see Figure 5b), a noticeable decrease in the intensity of this peak is observed already at 300 °C and 340 °C. This marks the onset of dehydroxylation: the loss of structural water and, as a result, the destruction of the crystal lattice. Such behavior may be associated with isomorphic substitutions in the octahedral layer, which reduce the structure's thermal stability. In contrast, montmorillonite clay from the IV layer of the Cherkasy deposit (see Figure 5c) exhibits significantly greater thermal stability of the structural OH groups. The peak around 3600 cm^{-1} in this sample remains practically unchanged, or decreases significantly less than in other samples, even at 300 °C and 340 °C. This indicates a more perfect, thermally stable crystal structure, which is probably due to a different nature of isomorphic substitutions or to their smaller number.

Based on these data, the clay of the IV layer of the Cherkasy deposit is best suited for use in iron ore pellet production. Pellet production involves high-temperature firing (over 1200 °C), and the binder (bentonite) must retain its properties for as long as possible. The higher the temperature at which dehydroxylation of the clay begins, the longer it retains its binding capacity and contributes to pellet strengthening. Delaying the destruction of the layered structure of montmorillonite to higher temperatures allows it to perform the binder function more effectively in the early stages of firing, preventing the disintegration of raw pellets until strong mineral bonds form between iron ore particles. Thus, the high thermal stability of the montmorillonite clay in the IV layer provides an advantage in the production of high-quality iron ore pellets.

Thermogravimetric analysis (TGA) was performed in the temperature range of 25–400 °C at a heating rate of 10 °C/min under an air atmosphere. The selected temperature interval corresponds to the dehydration range identified by XRD and IR spectroscopy (20–340 °C) and allows quantitative evaluation of water removal processes without interference from structural dehydroxylation occurring at higher temperatures.

The TG curves confirm a two-stage mass loss behavior. Up to 180–200 °C, physically adsorbed and interlayer water is removed. In the range of 250–360 °C, additional mass loss is associated with the release of channel water from palygorskite and the onset of structural water removal.

Clay minerals, such as montmorillonite, have a characteristic layered structure that appears microscopically as flaky or scaly particles, and their interaction and aggregation determine the overall porosity and texture of the material (see Figure 6).

Upon closer examination of Figure 6a, which shows the clay mixture of layers 2 and 3, one can observe mainly large, densely packed flaky aggregates. They often have an irregular, amoeba-like shape with clearly defined contours. Between these larger aggregates, gaps are visible, forming porosity, but the overall packing appears to be relatively dense and heterogeneous. Of particular note are the large and rounded formations in the central part of the image, which represent a compacted aggregate of clay particles. Overall, this mixture appears to be a fairly dense mass with large, possibly unevenly distributed aggregates, and the cavity space for water accumulation appears uneven.

In contrast, the image in Figure 6b, which illustrates a mixture of clays from layers 2 and 4, shows a noticeably different microstructure. Relatively smaller, more elongated, sometimes even needle-shaped or rod-shaped particles predominate here. These particles appear looser and less dense in aggregates compared to the upper image. The microstruc-

ture is more open and porous, with particles less densely arranged and forming a more branched network with numerous small and elongated cavities. The distribution of clay particles throughout the field of view appears more uniform, with less pronounced large, individual aggregates. Although there are one or two larger, more compact aggregates in the lower right corner, they do not dominate the overall picture as in the upper image.

Quantitative image analysis was performed using ImageJ software (version 1.54 g). The average aggregate size in the II + III mixture was 14.2 ± 3.1 μm, whereas in the II + IV mixture it was 6.8 ± 1.9 μm. The porosity estimated by image thresholding was 21% for the II + III mixture and 34% for the II + IV mixture. The finer particle distribution and higher open porosity explain the improved water retention and gas permeability of the IV-layer system.

Comparing these two microstructures, it can be concluded that the addition of layer 4 clay to layer 2 clay results in a significantly looser, more porous, and more uniform microstructure compared to the mixture of layers 2 and 3. Layer 3 clay may contribute to denser, potentially less plastic aggregates, which may not improve the mixture's homogeneity. In contrast, layer 4 clay is likely composed of smaller, more elongated particles that interact more readily, forming an open yet stable porous network. This morphology provides more efficient water retention in the pores, which is vital for the plasticity of the green pellets, and also provides better gas permeability, which is important during dehydration. This is fully consistent with the results of the previous IR analysis (see Figure 5), which showed higher thermal stability of the clay of the 4th layer.

In the context of iron ore pellet production, the microstructure of the binder clay is critically important. For green pellets, a more uniform, porous structure, as in the 2nd- and 4th-layer mix, provides better water retention and a more homogeneous distribution of clay in the charge, which contributes to the formation of strong, stable pellets. The presence of large, dense aggregates (as in the 2nd- and 3rd-layer mix) can create weak spots and inhomogeneities. For calcined pellets, a more open and uniform porous structure, characteristic of the 2nd and 4th layer mix, contributes to improved gas permeability, controlled shrinkage, and a lower probability of cracking, ultimately enhancing the strength, recoverability, and other metallurgical characteristics of the finished pellet. Thus, based on electron microscopy analysis, the mixture of clays from the 2nd and 4th layers exhibits a more desirable microstructure, making it the optimal component for binder mixtures in the production of high-quality iron ore pellets.

The average pore size in the II + III mixture was 18–35 μm, whereas in the II + IV mixture it decreased to 8–20 μm, indicating a more homogeneous capillary network.

The finer aggregates observed in the II + IV mixture increase the number of capillary contact points between iron ore particles. This enhances capillary cohesion during drying and reduces stress concentration, which explains the higher dry pellet strength observed experimentally.

3.2. Textural Characteristics of Binder Materials

Specific surface area and porosity were determined by nitrogen adsorption (BET method). The specific surface areas were:

- Kaolinite—18 m^2/g;
- Montmorillonite (II layer)—64 m^2/g;
- Montmorillonite (IV layer)—87 m^2/g.

The higher specific surface area of layer IV clay correlates with its increased adsorption capacity and explains the enhanced capillary bonding and mechanical strength.

Although specific surface area was determined using the BET method, detailed pore size distribution analysis (e.g., BJH method) was not performed in this study. Such analysis

would provide a more precise characterization of mesoporous structures and their contribution to capillary pressure and fluid transport. Therefore, the quantitative relationship between pore size distribution and mechanical strength remains an important direction for future research.

3.3. Study of the Adsorption Capacity of Charge Components for Pellet Production

In raw pellets, the role of the mineral binder is minimal due to the low-temperature nature of the pelletizing process, but its hydrophilicity is of significant importance.

To obtain new data in this direction, relevant studies were conducted on the dependence of strength parameters on the hydrophilicity of the additive, consisting of two stages: analysis of the adsorption capacity of the pellet feed components used in the raw pellet production process and the pelleting process itself.

Studies performed in the adsorber of PJSC "ArcelorMittal Kryvyi Rih" allowed us to obtain numerical values of the adsorption capacity of the above-mentioned binders:

concentrate of ore processing plant No. 2—2.09 J/g,
kaolinite—20.9 J/g,
montmorillonite of the II layer—71.13 J/g,
montmorillonite of the IV layer—92.05 J/g.

Next, the pellets were obtained using the aforementioned binding additives. In each experiment, which was repeated three times, the strength of 20 randomly selected pellets was determined (Tables 1–3).

Table 2. Comparison of obtained strength values with industrial requirements.

Type of Binder	Parameter	
	Green Pellet Strength, kg/Pellet	Dry Pellet Strength, kg/Pellet
Typical industrial requirement	≥1.5	≥5.0
Montmorillonite II layer	1.5	5.9
Montmorillonite IV layer	1.6–1.9	6.2–6.4

Table 3. Adsorption capacity and corresponding pellet strength values.

Type of Binder	Adsorption Capacity (J/g)	Green Pellet Strength (kg/Pellet)	Dry Pellet Strength (kg/Pellet)
Without binder	2.09	1.13	2.33
Kaolinite	20.9	1.33	3.80
Montmorillonite (II layer)	71.13	1.50	5.90
Montmorillonite (IV layer)	92.05	1.73	6.30

Analysis of the results (see Tables 1–3) allowed us to obtain a graphical relationship between the hydrophilicity of the binder additive (its adsorptive capacity) and the strength indicators of wet and dry pellets, as shown in Figure 7. The error bars are presented in Table 4.

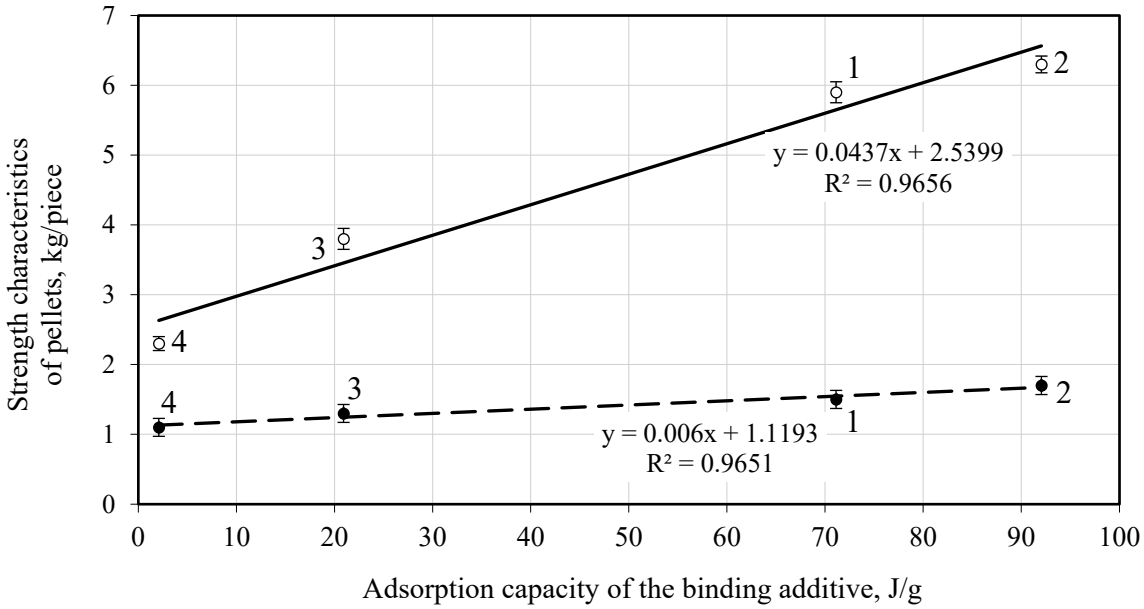

Figure 7. Dependence of the strength characteristics of wet (●) and dry (○) pellets on the adsorption capacity of the binder additive: 1—montmorillonite of the 2nd layer; 2—montmorillonite with palygorskite of the 4th layer; 3—kaolinite; 4—without additive (each point is the arithmetic mean of the results of three parallel experiments).

Table 4. Error bars.

Type of Binder	Parameter	
	Strength Characteristics of Pellets, kg/Pellet	**Error Bars, kg/Pellet**
	Wet pellets	
Without binder	1.13	±0.05
Kaolinite	1.33	±0.06
Montmorillonite II layer	1.50	±0.08
Montmorillonite IV layer	1.73	±0.08
	Dry pellets	
Without binder	2.33	±0.10
Kaolinite	3.80	±0.15
Montmorillonite II layer	5.90	±0.12
Montmorillonite IV layer	6.30	±0.15

To quantify the relationship between adsorption capacity (A, J/g) and pellet strength (S, kg/pellet), linear regression analysis was performed.

For green (wet) pellets, the regression equation can be expressed as:

$$S_{wet} = 1.1193 + 0.006A$$

with a coefficient of determination $R^2 = 0.9651$, indicating a strong positive correlation.

For dried pellets, the dependence is more pronounced:

$$S_{dry} = 2.5399 + 0.0437A$$

with $R^2 = 0.9656$, confirming an almost linear functional relationship.

For the green pellet regression model (S_{wet} = 1.1193 + 0.006A), the 95% confidence interval for the slope was [0.004–0.008].

For the dried pellet regression model (S_{dry} = 2.5399 + 0.0437A), the 95% confidence interval for the slope was [0.038–0.049].

It should be noted that the regression analysis is based on a limited number of experimental data points (n = 4 binder types). Although each point represents an average of multiple measurements (n = 60 pellets), the small number of independent variables restricts the robustness and generalizability of the statistical model. The high coefficient of determination ($R^2 > 0.96$) observed in this study may partially reflect the constrained dataset rather than a universally linear relationship. Future work should include a broader range of binder compositions and concentrations to validate the proposed correlation and assess potential non-linear behavior.

The relatively narrow confidence intervals further confirm the stability of the regression estimates.

The statistical significance of the regression models was verified using ANOVA. For green pellets, the regression model was significant (F-test, $p < 0.01$). For dried pellets, the model also demonstrated high statistical significance ($p < 0.01$), confirming that adsorption capacity is a reliable predictor of pellet strength.

Each experimental point represents the arithmetic mean of three independent experiments (n = 60 pellets). The standard deviation did not exceed $\pm$0.08 kg/pellet for green pellets and $\pm$0.15 kg/pellet for dried pellets. The differences between the montmorillonite of layer IV and other binders were statistically significant ($p < 0.05$, Student's *t*-test).

The high R^2 values confirm that adsorption capacity acts as a key controlling factor within the investigated system, showing a strong correlation with pellet strength, although it should not be interpreted as the sole determinant of mechanical performance.

While the obtained regression models demonstrate a strong statistical relationship between adsorption capacity and pellet strength, it is important to recognize that pellet strength is a multifactorial property. In addition to adsorption phenomena, parameters such as particle size distribution, surface energy, wettability, rheological behavior of the pelletizing mixture, and structural rearrangements during drying also contribute to the final mechanical properties. Therefore, adsorption capacity should be considered as a dominant, but not exclusive, factor within the studied experimental domain.

To further strengthen the statistical validity of the results, Pearson correlation coefficients (r) were calculated. For green pellets, r = 0.982 ($p < 0.01$), and for dried pellets, r = 0.983 ($p < 0.01$), indicating a very strong positive linear correlation between adsorption capacity and pellet strength.

One-way ANOVA confirmed that the differences in pellet strength between binder types are statistically significant ($p < 0.05$). The regression models were also statistically significant, with *p*-values below 0.01, confirming the reliability of the established relationships.

The 95% confidence intervals for the regression coefficients were calculated, confirming that the slope values remain positive within the confidence intervals, supporting the robustness of the proposed quantitative model.

The obtained dependencies clearly demonstrate the main trends: the strength of wet pellets and that of dried pellets increase with increasing adsorption capacity of the additive. However, the effect of adsorption capacity is much more pronounced for dried pellets.

Based on the results obtained, a schematic representation of the stages of pellet strengthening was created (Figure 8).

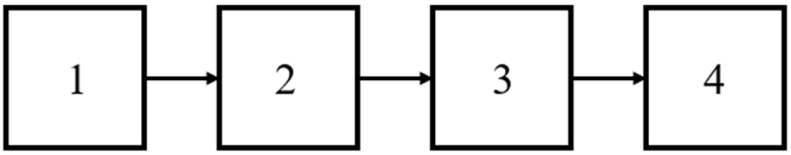

Figure 8. Schematic representation of pellet strengthening stages: (1) adsorption film formation on ore particles; (2) capillary bridge development; (3) controlled dehydration of montmorillonite–palygorskite; (4) formation of stable interparticle contacts.

When analyzing the strength characteristics of wet pellets, it is evident that without a binder (point 4), their strength is the lowest, at about 1.1 kg/pellet. With the addition of kaolinite (point 3), whose adsorption capacity is about 20 J/g, the strength of raw pellets increases slightly to about 1.3 kg/pellet. The use of montmorillonite in the 2nd layer (point 1), with an adsorption capacity of about 70 J/g, leads to a moderate increase in strength to 1.5 kg/pc. The highest strength among wet pellets, approximately 1.7 kg/pellet, is demonstrated by the combination of montmorillonite with palygorskite of the 4th layer (point 2), which has the highest adsorption capacity of about 95 J/g. In general, the strength range for wet pellets is relatively narrow, indicating a moderate influence of additive adsorption capacity at this stage.

In contrast, the strength characteristics of dried pellets exhibit significantly greater sensitivity to the binder additive's adsorption capacity. For them, there is an almost linear, significant increase in strength over a wide range, indicating the additive's adsorption capacity plays a significant role in determining the final strength. Montmorillonite with palygorskite of the 4th layer stands out in particular. Its significantly higher adsorption capacity and ability to provide the highest strength indicators for both wet and dried pellets may be due to the synergistic effect of the presence of fibrous palygorskite and the special mineralogical and morphological composition of the 4th layer clay layer, which contributes to better water retention capacity and more effective interaction with ore particles.

From a scientific point of view, this dependence confirms the importance of clay minerals' adsorption capacity as binding agents in agglomeration processes. Additives with high adsorption capacity can form stronger capillary and interparticle bonds in wet pellets and, after drying, form stable microstructures through crystal bridges or other strengthening mechanisms, thereby significantly improving the mechanical properties of the final product.

3.4. Influence of Charge Moisture

An increase in charge moisture from 8.5% to 9.5% resulted in a non-linear variation in green pellet strength. At 9% moisture, maximum strength was observed. Excess moisture reduced capillary pressure due to pore flooding, whereas insufficient moisture limited liquid bridge formation. The effect was most stable for layer IV clay, demonstrating lower sensitivity to moisture fluctuations, which is industrially advantageous.

4. Discussion

The strengthening of pellets in the "clay mineral—iron ore concentrate" system can be explained by the sequential evolution of interparticle interactions during pellet formation and drying. At the green stage, cohesion is governed primarily by adsorption and capillary effects:

$$P_c = 2\gamma\cos\theta / r$$

where P_c is the capillary pressure, γ is the surface tension of the liquid phase, θ is the contact angle, and r is the effective pore radius.

According to this relationship, capillary pressure increases inversely with pore radius, which provides a theoretical explanation for the experimentally observed increase in pellet strength with decreasing pore size and increasing specific surface area. The finer and more homogeneous pore structure observed in the montmorillonite–palygorskite system (layer IV) leads to higher capillary pressures during drying, resulting in stronger interparticle bonding.

Furthermore, the extended dehydration interval associated with palygorskite ensures a gradual reduction in liquid bridges, preventing abrupt capillary collapse and reducing internal stress development. This combination of structural and thermodynamic effects explains the superior mechanical performance of the composite binder system.

Clay minerals with high specific surface area preferentially adsorb water and form stable hydration films on particle surfaces, which promote the formation of liquid bridges and enhance capillary bonding between iron oxide grains. The higher the adsorption capacity of the binder, the more stable and uniformly distributed these interparticle bonds become.

The obtained linear relationship between adsorption capacity and pellet strength is consistent with the capillary bonding mechanism described by Forsmo [18–20], who emphasized the role of liquid bridges in green pellet cohesion. However, the slope of the regression model obtained in the present work is higher, which can be attributed to the presence of fibrous palygorskite, which enhances capillary reinforcement.

Similar conclusions regarding the importance of binder hydration behavior were reported by Kawatra and co-authors [7,10,21], who demonstrated that swelling capacity governs pellet durability during drying. In comparison, the present study provides a quantitative statistical confirmation of this mechanism.

Furthermore, the influence of binder type on compressive strength agrees with the findings of U. Srivastava et al. [24], although the enhanced performance observed here highlights the additional structural contribution of montmorillonite–palygorskite systems.

During drying, the gradual removal of physically adsorbed and interlayer water results in densification of the pellet structure and closer particle packing. The kinetics of dehydration, including activation energy and rate constants associated with water removal from interlayer and channel structures, were not quantitatively determined in this study. Such parameters could be evaluated using advanced thermogravimetric analysis combined with kinetic modeling. Incorporating kinetic analysis would provide a deeper understanding of the temporal evolution of capillary forces and structural transformations during drying. In montmorillonite containing palygorskite, dehydration occurs over a broad temperature range, providing controlled moisture release and reducing the development of internal stress. This results in a more homogeneous microstructure and a significant increase in dry pellet strength.

At elevated temperatures, the binder maintains structural integrity long enough to preserve the pellet framework before partial structural transformations occur. The higher thermal stability of the IV-layer clay contributes to improved resistance to structural collapse and supports stable interparticle contacts.

The synergistic effect of montmorillonite and palygorskite can be interpreted at the microstructural and molecular levels. Montmorillonite, characterized by a layered structure and high swelling capacity, provides extensive adsorption sites and promotes the formation of hydration films and capillary bridges. In contrast, palygorskite exhibits a fibrous morphology with channel-type porosity, contributing to structural reinforcement and directional connectivity within the binder network.

The combination of these two mineral phases results in a hybrid microstructure where layered adsorption-controlled interactions are complemented by fibrous mechanical stabilization. Additionally, the presence of different water-binding environments (inter-

layer water in montmorillonite and channel water in palygorskite) leads to a broadened dehydration interval, which stabilizes the evolution of capillary forces during drying. This multi-scale interaction explains the observed improvement in both green and dry pellet strength.

Thus, pellet strengthening represents a continuous transition from adsorption-controlled cohesion in green pellets to consolidated solid contacts after drying. The superior performance of montmorillonite with palygorskite is attributed to its high adsorption capacity, extended dehydration interval, and favorable microstructural organization.

The results obtained in this study are specific to the investigated iron ore concentrate and clay materials from the Cherkasy deposit. Variations in mineral composition, particle size distribution, and surface chemistry may significantly affect adsorption behavior and pellet strength. Therefore, direct extrapolation of the results to industrial systems should be performed with caution. Further studies involving different raw materials and pilot-scale testing are required to confirm the scalability of the proposed approach.

The implementation of montmorillonite–palygorskite binders in industrial pellet plants could reduce bentonite consumption by 15–25% while maintaining green and dry pellet strength above industrial standards. The potential reduction in bentonite consumption (estimated at 15–25%) is based on the comparative analysis of pellet strength achieved with the montmorillonite–palygorskite system relative to conventional binders. However, this estimation remains preliminary and is derived from laboratory-scale experiments. Industrial validation, including pilot-scale pelletizing tests and process integration analysis, is required to confirm the practical feasibility of such reductions. This may lead to improved process stability and reduced production costs in large-scale agglomeration systems.

Thus, despite the trends in the use of new binders [39], traditional bentonite clay remains and will remain an important component of the modern technological process of pellet production due to its widespread resource base, proven application technology, and low cost [40,41].

The present study has several limitations that should be acknowledged. First, the experimental analysis was conducted using a single type of iron ore concentrate, which limits the general applicability of the results to other raw material systems. Second, the number of investigated binder types was limited, and the statistical model is based on a relatively small dataset. Third, high-temperature processes, including roasting and phase transformations, were not considered. Finally, the absence of detailed pore size distribution analysis restricts the ability to fully quantify capillary effects. These limitations define the scope of applicability of the obtained results and indicate directions for future research.

5. Conclusions

Thus, the obtained research results, combined with previous analyses of IR spectra (which demonstrated higher thermal stability of the 4th layer clay) and electron microscope images (which showed a more optimal microstructure of the mixture with the clay of the 4th layer), consistently confirm that montmorillonite with palygorskite of the 4th layer is the most effective composite binding additive for the production of iron ore pellets. Its high adsorption capacity directly translates into excellent pellet strength, which is critical for subsequent heat treatment.

The gradual removal of water molecules from the binder additive, associated with the wider dehydration limits of palygorskite, can significantly prolong the duration of the pellet “shock” effect.

The higher efficiency of layer IV montmorillonite enables a potential reduction in binder consumption of 15–25% while maintaining the required strength. Considering typical industrial bentonite consumption of 8–10 kg per ton of pellets, this could yield

savings of 1.5–2.5 kg/t, resulting in significant annual cost reductions for large-scale pellet plants.

Adsorption capacity of composite clay minerals is a governing parameter controlling both green and dry pellet strength, as confirmed by statistically significant regression models ($R^2 > 0.96$). Montmorillonite–palygorskite mixtures demonstrate extended dehydration behavior, providing gradual moisture release and improved structural stability during drying. Microstructural organization, including aggregate size reduction and increased open porosity, enhances capillary bonding and gas permeability of pellets. From an industrial perspective, the use of montmorillonite–palygorskite binders enables potential reduction in bentonite consumption while maintaining pellet strength above industrial requirements.

Author Contributions: Conceptualization, Y.C., I.T., N.H. and K.S.; methodology, Y.C. and D.M.; investigation, K.S., Y.C., L.L., M.S. and A.M.; data curation, K.S. and I.T.; writing—original draft preparation, Y.C., D.M., K.S..; writing—review and editing, I.T., N.H. and D.M.; visualization, K.S., L.L., M.S. and A.M.; supervision, D.M.; project administration, Y.C. and D.M. All authors have read and agreed to the published version of the manuscript.

Funding: This research received no external funding.

Data Availability Statement: The raw data supporting the conclusions of this article will be made available by the authors on request.

Conflicts of Interest: The authors declare no conflict of interest.

References

1. Liu, Y.; Jiao, K.; Zhang, J.; Wang, C.; Zhang, L.; Fan, X. Research progress and future prospects in the service security of key blast furnace equipment. *Int. J. Miner. Metall. Mater.* **2024**, *31*, 2121–2135. [CrossRef]
2. Wang, B.; Wang, W.; Chen, X.; Chen, L.; Wang, J.; Chen, S. Reduction Behaviour and Microstructural Evolution Mechanism of Pellets Based on Blast Furnace Dissection. *Metall. Mater. Trans. B* **2025**, *56*, 1994–2008. [CrossRef]
3. Agrawal, A. Enhanced Stockline Measurement and Burden Descent Monitoring for Sustainable Blast Furnace. *J. Sustain. Metall.* **2025**, *11*, 1778–1788. [CrossRef]
4. Miroshnichenko, D.; Shmeltser, K.; Kormer, M. Factors Affecting the Formation the Carbon Structure of Coke and the Method of Stabilizing Its Physical and Mechanical Properties. *C* **2023**, *9*, 66. [CrossRef]
5. Miroshnichenko, D.; Shmeltser, K.; Kormer, M.; Bannikov, L.; Nedbailo, S.; Miroshnychenko, M.; Mukina, N.; Shved, M. Formation of Improved Metallurgical Properties and Carbon Structure of Coke by Optimizing the Composition of Petrographically Heterogeneous Interbasin Coal Batches. *C* **2025**, *11*, 69. [CrossRef]
6. Miroshnichenko, D.; Shmeltser, K.; Kormer, M.; Sahalai, D.; Pyshyev, S.; Kukhar, O.; Korchak, B.; Chervinskyy, T. Influence of Raw Materials and Technological Factors on the Sorption Properties of Blast-Fuel Coke. *ChemEngineering* **2024**, *8*, 30. [CrossRef]
7. Miroshnichenko, D.; Shmeltser, K.; Kormer, M.; Soloviov, Y.; Pyshyev, S.; Korchak, B.; Shved, M.; Prysiazhnyi, Y. Electrical Resistance as an Aggregate Characteristic of Coke Properties for Electrochemical and Coke Production. *Electrochem* **2024**, *5*, 258–273. [CrossRef]
8. Miroshnichenko, D.; Shmeltser, K.; Kormer, M.; Sytnyk, O.; Avdeyuk, I.; Miroshnychenko, M.; Shved, M. Using Coal Resources with Optimal Bursting Pressure for the Production of High-Quality Metallurgical Coke. *Resources* **2025**, *14*, 70. [CrossRef]
9. Eisele, T.C.; Kawatra, S.K. A review of binders in iron ore pelletization. *Miner. Process. Extr. Metall. Rev.* **2003**, *24*, 1–90. [CrossRef]
10. Kawatra, S.K.; Claremboux, V. Iron Ore Pelletization: Part II. Inorganic Binders. *Miner. Process. Extr. Metall. Rev.* **2021**, *43*, 813–832. [CrossRef]
11. Claremboux, V.; Kawatra, S.K. Iron Ore Pelletization: Part III. Organic Binders. *Miner. Process. Extr. Metall. Rev.* **2022**, *44*, 138–154. [CrossRef]
12. Haas, L.A. *Effectiveness of Organic Binders for Iron Ore Pelletization*; Department of the Interior: Washington, DC, USA, 1989; 21p.
13. Kawatra, S.K.; Claremboux, V. Iron Ore Pelletization: Part I. Fundamentals. *Miner. Process. Extr. Metall. Rev.* **2021**, *43*, 529–544. [CrossRef]
14. Bhuiyan, I.U.; Mouzon, J.; Schröppel, B.; Kaech, A.; Dobryden, I.; Forsmo, S.P.; Hedlund, J. Microstructure of Bentonite in Iron Ore Green Pellets. *Microsc. Microanal.* **2014**, *20*, 33–41. [CrossRef]
15. Liu, Z.R.; Ye, W.-M.; Zhu, J.-C.; Chen, Y.-G.; Wang, Q. Temperature and alkaline solution effects on the hydro-mechanical behaviours of GMZ bentonite pellet mixtures. *Acta Geotech.* **2023**, *18*, 6097–6110. [CrossRef]

16. Liu, X.D.; Lu, X.J.; Qiu, J.; Wang, Z.M.; Wu, P. Purification of Low Grade Ca-Bentonite for Iron Ore Pellets. *Adv. Mater. Res.* **2012**, *454*, 237–241. [CrossRef]
17. Toporov, N.I.; Prosvirov, S.N.; Gritsenko, G.B. Preparation of powdered bentonite for the production of iron-ore pellets. *Metallurgist* **1986**, *30*, 81–82. [CrossRef]
18. Kawatra, S.K.; Ripke, S.J. Developing and understanding the bentonite fiber bonding mechanism. *Miner. Eng.* **2001**, *14*, 647–659. [CrossRef]
19. Gasik, M.I.; Uchitel, A.D.; Panchenko, A.N.; Khmel, V.V.; Solov'EV, E.D. Wear of Lurgi-552 gratings when roasting pellets with alkaline bentonite binder. *Steel Transl.* **2009**, *39*, 28–33. [CrossRef]
20. Villanueva, A.; Hoff, S.; Michailovski, A. BASF novel iron ore binder technology: Study of bentonite modification. In Proceedings of the 5th Brazilian Symposium on Agglomeration of Ores (Simpósio Brasileiro de Aglomeração de Minérios), São Paulo, Brazil, 26–28 October 2017. [CrossRef]
21. Forsmo, S.P.E.; Apelqvist, A.; Björkman, B.; Samskog, P.-O. Binding mechanisms in wet iron ore green pellets with a bentonite binder. *Powder Technol.* **2006**, *169*, 147–158. [CrossRef]
22. Forsmo, S.P.E.; Vuori, J.P. The determination of porosity in iron ore green pellets by packing in silica sand. *Powder Technol.* **2005**, *159*, 71–77. [CrossRef]
23. Tsukerman, T.; Duchesne, C.; Hodouin, D. On the drying rates of individual iron oxide pellets. *Int. J. Miner. Process.* **2007**, *83*, 99–115. [CrossRef]
24. Kawatra, S.K.; Ripke, S.J. Effects of bentonite fiber formation in iron ore pelletization. *Int. J. Miner. Process.* **2002**, *65*, 141–149. [CrossRef]
25. Ripke, S.J.; Kawatra, S.K. Bentonite binder effective strength (BESt) test for unfired iron ore pellets. *Min. Metall. Explor.* **2004**, *21*, 65–70. [CrossRef]
26. Desai, R.R.; Erwin Desa, J.A.; Aswal, V.K. Hydration studies of Bentonite clay. In Proceedings of the 56th DAE Solid State Physics Symposium, SRM University, Kattankulathur, Tamilnadu, India, 19–23 December 2011; pp. 197–198. [CrossRef]
27. Srivastava, U.; Kawatra, S.K.; Eisele, T.C. Study of Organic and Inorganic Binders on Strength of Iron Oxide Pellets. *Metall. Mater. Trans. B* **2013**, *44*, 1000–1009. [CrossRef]
28. Ngara, T.; Mavengere, S.; Bright, S.; Mapamba, L. Investigating the effectiveness of organic binders as an alternative to bentonite in the pelletization of low grade iron ore. *Physicochem. Probl. Miner. Process.* **2023**, *59*, 176094. [CrossRef]
29. Khalifa, A.; Abdel Hamid, E.M. Physical Purification of Egyptian Bentonite and Its Application as a Sustainable Binder in Iron Oxide Waste Recycling. In *Clay Science—Bridging Geology and Physical Chemistry*; IntechOpen: London, UK, 2025. [CrossRef]
30. Al-Hammood, A.A.; Frayyeh, Q.J.; Abbas, W.A. Raw bentonite as supplementary cementitious material—A review. *J. Phys. Conf. Ser.* **2021**, *1795*, 012018. [CrossRef]
31. Pieter le Roux, H.; Görgens, J.F.; Tyhoda, L.; Louw, T.M.; Akdogan, G. The use of spent liquors from paper and pulp industry as binders for the pelletization of chromite fines. *Miner. Eng.* **2024**, *216*, 108846. [CrossRef]
32. Ma, K.; Zhang, S.; Zhang, J.; Pu, T.; Yin, C.; Chen, M.; Rao, J.; Bai, C. Strength variation of green pellets and pelletizing mechanism in the pelletization process of vanadium–titanium iron concentrate using organic binders. *Powder Technol.* **2025**, *452*, 121434. [CrossRef]
33. Christidis, G.E. Origin of the Bentonite Deposits of Eastern Milos, Aegean, Greece: Geological, Mineralogical and Geochemical Evidence. *Clays Clay Miner.* **1995**, *43*, 63–77. [CrossRef]
34. Sastry, K.V.; Fuerstenau, D.W. Laboratory studies on the batch balling kinetics of taconite concentrates. In Proceedings of the 9th International Mineral Processing Congress, Prague, Czech Republic, 1–6 June 1970; pp. 55–69.
35. Day-Stirrat, R.J.; Bryndzia, L.T. Hydration behavior by X-ray diffraction profile fitting of smectite-bearing minerals. *E3S Web Conf.* **2020**, *205*, 04009. [CrossRef]
36. Sharma, V.K.; Prabhudesai, S.A.; Dessai, R.R.; Desa, J.A.E.; Mitra, S.; Mukhopadhyay, R. Diffusion of water in bentonite clay: Neutron scattering study. In Proceedings of the 57th DAE Solid State Physics Symposium, Indian Institute of Technology, Bombay, Mumbai, India, 3–7 December 2012; pp. 918–919. [CrossRef]
37. Orolínová, Z.; Mockovčiaková, A.; Dolinská, S.; Briančin, J. Effect of thermal treatment on the bentonite properties. *Arch. Tech. Sci.* **2012**, *4*, 49–56. [CrossRef]
38. Praetorius, S.; Schößer, B. Bentonite and bentonite suspensions. In *Bentonite Handbook*; Wiley: Weinheim, Germany, 2017; pp. 9–20. [CrossRef]
39. Parathodiel, H.; Mousa, E.; Ahmed, H.; Elsadek, M.; Forsberg, K.; Andersson, C. Developing Iron Ore Pellets Using Novel Binders for H2-Based Direct Reduction. *Sustainability* **2023**, *15*, 11415. [CrossRef]

40. Schoch, K.; Liedtke, C.; Bienge, K. Designing on the Basis of Recycling-Metallurgy Possibilities: Material-Specific Rules and Standards for "Anti-Dissipative" Products. *Resources* **2021**, *10*, 5. [CrossRef]
41. Manu, K.; Mousa, E.; Ahmed, H.; Elsadek, M.; Yang, W. Maximizing the Recycling of Iron Ore Pellets Fines Using Innovative Organic Binders. *Materials* **2023**, *16*, 3888. [CrossRef] [PubMed]